# IV

Publication IV

J. Oksanen and J. Tulkki, *Fast coherent all-optical flip-flop memory*, Applied Physics Letters **88**, pp. 181118-1-181118-3 (2006).

# Fast coherent all-optical flip-flop memory

Jani Oksanen[a] and Jukka Tulkki
*Laboratory of Computational Engineering, Department of Electrical and Communications Engineering, Helsinki University of Technology, P.O. Box 9203, FIN-02015 HUT, Finland*

(Received 16 August 2005; accepted 29 March 2006; published online 5 May 2006)

Coherent nonlinear feedback is shown to eliminate the most critical transient problems in the known active integrated all-optical flip-flop structures, potentially increasing the operating speed by an order of magnitude. The nonlinearity is based on the interference of two coherent optical fields and on operating the pertinent laser amplifiers only above the laser threshold. Therefore the lasers have an approximately constant carrier density and an ever present photon population in the laser mode. This enables fast switching. Numerical analysis based on coupled rate equations demonstrates switching times below 25 ps (40 GHz). © *2006 American Institute of Physics*.
[DOI: 10.1063/1.2199971]

Although a simple task in the electronic domain, realizing memory circuits in the optical domain has turned out to be very challenging. The recent intensive research on photonic crystals and related technologies has provided innovative solutions in manipulating and controlling the flow of light.[1–3] However, the development of the basic building blocks needed for optical computing, the fast integrated optical memory and logic, is still at its infancy. The last two decades have witnessed the proposal of many all-optical flip-flop constructions based on active devices.[4–11] Many of the otherwise promising structures rely on turning on and off a laser field. This slows down their operation. A recently demonstrated integrated flip-flop memory based on two coupled microring lasers has shown very promising switching characteristics, even if the lasers still operate on both sides of the lasing threshold.[12]

This work introduces a way of realizing the nonlinear feedback in a bistable system composed of two gain clamped semiconductor optical amplifiers (laser amplifiers). In the resulting flip-flop structure, the coherent optical flip-flop (COFF), the lasers stay well above the lasing threshold at all times and thus the changes in the carrier densities are minimized. This reduces the transient times drastically.

A simple model for the COFF composes of two laser amplifiers, bandstop filters, external reference lasers, and two optical isolators (Fig. 1). The isolators are used in the schematic representation for simplicity. In the calculations they are replaced with active antireflector structures.

The two current driven laser amplifiers (marked as $L_1$ and $L_2$ in Fig. 1) playing the key role in the operation share three common optical modes, denoted by wavelengths $\lambda_1$, $\lambda_2$, and $\lambda_3$. In laser $L_1$ the lasing occurs at $\lambda_1$ and in laser $L_2$ at $\lambda_2$. Modes that are not lasing ($\lambda_2$ and $\lambda_3$ in $L_1$ and $\lambda_1$ and $\lambda_3$ in $L_2$) have larger losses. Therefore there is optical power in these modes only if it is originally injected by an external field. Both lasers are phase locked to external master lasers (also operating at wavelengths $\lambda_1$ and $\lambda_2$, respectively).

The nonlinear coupling between the lasers is formed so that wavelength $\lambda_1$ from laser $L_1$ is made to interfere with the coherent bias field $E_{B1}$ and then guided to $L_2$. Wavelength $\lambda_2$ from $L_2$, similarly interfering with the bias signal $E_{B2}$, is fed back to $L_1$. The interference (a nonlinear process in terms of optical power) combined with the linearly decreasing output power of the laser mode of a laser amplifier (a linear process in terms of optical power) provides the means for nonlinear coupling between the lasers.

When the nonlinear coupling between the lasers is carefully adjusted, a bistable system suitable for flip-flop operation is formed. In the stable state denoted as the set state, $L_1$ has a few tens of percent of the optical power in the laser mode ($\lambda_1$) and the rest in the feedback mode ($\lambda_2$). The resulting feedback to $L_2$, however, is approximately zero after accounting for the interference, and $L_2$ correspondingly has approximately all of its power in the laser mode ($\lambda_2$). The reverse situation is denoted as the reset state.

Injecting an external signal at $\lambda_3$ to laser $L_1$ (set operation) changes the stability conditions so that only the set state is possible and the system must move to this state. Similarly, injecting an external signal to $L_2$ resets the COFF.

The rate equations describing the COFF are written using vector representations for the carrier densities $\mathbf{n}$ and the complex electric fields $\mathbf{E}_j$. There is one vector component for each laser in the COFF and the three vectors $\mathbf{E}_j$ ($j \in \{U,B,C\}$) describe the propagating fields in the three cavity modes ($U$ for the field in mode $\lambda_1$, $B$ in $\lambda_2$, and $C$ in $\lambda_3$). The use of complex electric fields instead of the con-

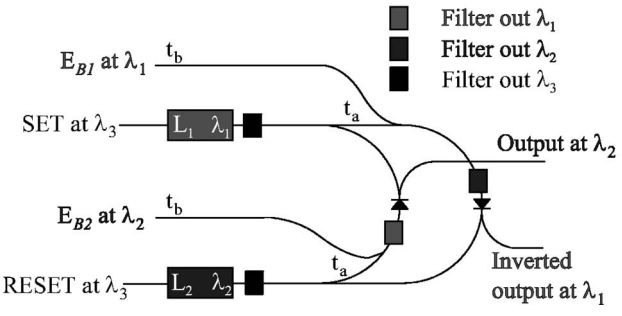


FIG. 1. A schematic representation of the COFF with the two lasers $L_1$ and $L_2$ acting as the core of the flip-flop. Injecting light in the set and reset ports sets and resets the flip-flop, respectively. The output and the inverted output can be read from the respective output ports. The bias fields $E_{B1}$ and $E_{B2}$ are coherent fields obtained from two master lasers. In the calculations optical isolators, used here for simplicity, are replaced by interferometric antireflectors suitable for optical integration.

[a]Electronic mail: jani.oksanen@lce.hut.fl

 

TABLE I. The parameter values used in the calculations.

| Symbol | Value | Comment |
|---|---|---|
| $I$ | 4.2 mA | Injection current |
| $V$ | 9 $\mu$m$^3$ | Volume of the optical cavity |
| $L$ | 10 $\mu$m | Length of the cavity |
| $n_r$ | 3 | Refractive index |
| $v$ | $10^8$ m s$^{-1}$ | Speed of light |
| $\tau$ | 1 ns | Carrier lifetime |
| $\hbar\omega$ | 1 eV | Photon energy |
| $G_{\max}$ | $10^5$/m | Maximum gain |
| $n_{\text{nom}}$ | $10^{22}$ m$^{-3}$ | Transparency carrier density |
| $\epsilon$ | $10^{-23}$ m$^3$ | Gain compression factor |
| $\alpha_L$ | 10 536/m | Loss coefficient for the lasing mode |
| $\alpha_s$ | 25 848/m | Loss coefficient for the other modes |
| $T_L$ | 0.1 | Reflectivity for power at laser mode |
| $T_s$ | 0.228 | Reflectivity for power at signal mode |
| $\xi$ | $1/2\hbar\omega v\sqrt{\varepsilon/\mu}$ | $\xi\lvert E \text{ field}\rvert^2 \rightarrow$ photon density |
| $\alpha_{\text{lef}}$ | 0–0.5 | Linewidth enhancement factor |
| $t_A$ | $\mathrm{I}\phi_0$ | Waveguide transmission coefficient ($E$ field) |
| $t_B$ | $-0.808\phi_0$ | Waveguide transmission coefficient ($E$ field) |
| $t_C$ | $2\times10^{-2}\phi_0$ | Waveguide transmission coefficient ($E$ field) |
| $g_A$ | 8 | Feedback gain (for $E$ field) |
| $\phi_0$ | $(1+i\alpha_{\text{lef}})/(1+i\alpha_{\text{lef}})$ | Waveguide phase shift |

ventional photon densities of the rate equations is necessary to account for the phase dependence of the interference. This gives the equations a highly nonlinear nature. The equations are quite similar in appearance to the rate equations describing a single phase locked laser[13] from which the model is derived:

$$\frac{d\mathbf{n}}{dt} = \frac{I}{qV} - \sum_{j\in\{U,B,C\}} 2\xi v\mathbf{G}_j(\mathbf{n})|\mathbf{E}_j|^2 - \frac{\mathbf{n}}{\tau}, \tag{1}$$

$$\frac{d\mathbf{E}_j}{dt} = \frac{v}{2}[\mathbf{G}_j(\mathbf{n}) - \alpha_j + i\Delta\omega_j(\mathbf{n})]\mathbf{E}_j + \frac{v}{2L}\mathbf{E}_j^{\text{ext}} + \frac{v}{2L}\mathbf{M}_j\mathbf{E}_j. \tag{2}$$

Explanations and values of the parameters are given in Table I below. The absolute value in Eq. (1) is applied to each component of $\mathbf{E}_j$ independently. The cavity losses for the mode $j$ are collected in the diagonal matrices $\alpha_j$. $\mathbf{E}_j^{\text{ext}}$ is a vector describing the fields injected from outside the cavity. The coupling matrices $\mathbf{M}_j$ are off-diagonal and describe the coupling between the lasers.

The diagonal elements of the modal gain matrix $\mathbf{G}_j(\mathbf{n})$ are given by

$$[\mathbf{G}_j(\mathbf{n})]_{m,m} = G_{\max}\frac{\mathbf{n}_m - n_{\text{nom}}}{(\mathbf{n}_m + n_{\text{nom}})[1 + 2\xi\epsilon|(\mathbf{E}_j)_m|^2]} \tag{3}$$

and the elements of the matrices containing the displacements of the frequency of the mode $j$ from the corresponding cavity resonance $\Delta\omega_j(\mathbf{n})$ by

$$[\Delta\omega_j(\mathbf{n})]_{m,m} = \alpha_{\text{lef}}[\Delta\mathbf{G}_j(\mathbf{n})]_{m,m}, \tag{4}$$

where $[\Delta\mathbf{G}_j(\mathbf{n})]_{m,m}=[\mathbf{G}_j(\mathbf{n})]_{m,m}-G_{\text{ref}}$ is the change in the gain with respect to the reference gain at which $[\Delta\omega_j(\mathbf{n})]_{m,m}$ are zero for the signal frequency. The reference gain is set to $G_{\text{ref}}=\alpha_L$.

Most of the parameter values in Table I are typical of semiconductor lasers. A few values (most notably $G_{\max}$, $n_{\text{nom}}$, and $\alpha_{\text{lef}}$), however, are better than typical.

In the calculations a more complete model than what is shown in Fig. 1 is used. The computational COFF model includes the two master lasers providing the bias and phase locking signals and replaces each optical isolator with a laser and an interferometer forming an active antireflector. The coupling matrices describing this model are given by

$$\mathbf{M}_U = \begin{bmatrix} 0 & C & iC & iB & B & 0 \\ C & 0 & 0 & iA & A & 0 \\ iC & 0 & 0 & 0 & 0 & 0 \\ iB & iA & 0 & 0 & 0 & 0 \\ B & A & 0 & 0 & 0 & 0 \\ 0 & 0 & 0 & 0 & 0 & 0 \end{bmatrix}, \tag{5}$$

$$(\mathbf{M}_B)_{m,n} = (\mathbf{M}_U)_{7-m,7-n}, \tag{6}$$

$$\mathbf{M}_C = 0, \tag{7}$$

$$A = \sqrt{T_L T_s} g_A t_A^2/4, \tag{8}$$

$$B = \sqrt{T_L T_s} g_A t_A t_B/(4\sqrt{2}), \tag{9}$$

$$C = T_L t_C/2, \tag{10}$$

where parameters $A$, $B$, and $C$ denote the coupling strength of the feedback, bias, and phase locking fields, respectively. The vectors describing the external injection are zero, except for $\mathbf{E}_C^{\text{ext}}=[0\ s_U(t)\ is_U(t)\ is_B(t)\ s_B(t)\ 0]^{\mathrm{T}}$, where $s_U(t)$ and $s_B(t)$ are the set and reset signals injected into the lasers. The loss matrices $\alpha_j$ are diagonal and given by $\alpha_U=\text{diag}[\alpha_L\ \alpha_L\ \alpha_L\ \alpha_s\ \alpha_s\ \alpha_s]$, $\alpha_B=\text{diag}[\alpha_s\ \alpha_s\ \alpha_s\ \alpha_L\ \alpha_L\alpha_L]$, and $\alpha_C=\text{diag}[\alpha_s\ \alpha_s\ \alpha_s\ \alpha_s\ \alpha_s\ \alpha_s]$, where the operator diag constructs a diagonal matrix from the vector following it. The elements 1 and 6 of the matrices and vectors are associated with the master lasers, elements 2 and 5 with lasers $\mathrm{L}_1$ and $\mathrm{L}_2$, and 3 and 4 with the lasers in the antireflectors.

The steady states of the COFF can also be found analytically by simplifying the steady state versions of Eqs. (1) and (2). This, however, is out of scope here and will be discussed in a separate work. Analytical studies were also used to determine some parameter values essential for operation and to minimize the effect of chirp to the steady state characteristics.

The fast operation of the COFF when sending short pulses to the set and reset ports is shown in Fig. 2(a). A pulse of only 25 ps (40 GHz) long is able to change the state. A nonzero value of $\alpha_{\text{lef}}$ slightly decreases the rise time, but also introduces small relaxation oscillations like fluctuations in the output. The switching threshold is studied in Fig. 2(b), showing the response to a sequence of set pulses, growing linearly in power. When the input power increases to a threshold value of 0.2 mW, the state is set.

The development of the internal state of the laser $\mathrm{L}_1$ is presented in Fig. 3, where the power (a) and phase (b) of the electric field of the laser mode $\lambda_1$ and the carrier density (c) in laser $\mathrm{L}_1$ are plotted when the COFF is operated by the pulses shown in Fig. 2(a). The change in the input to the system is compensated by the changes in the carrier density and in the optical power and phase of the laser mode. When

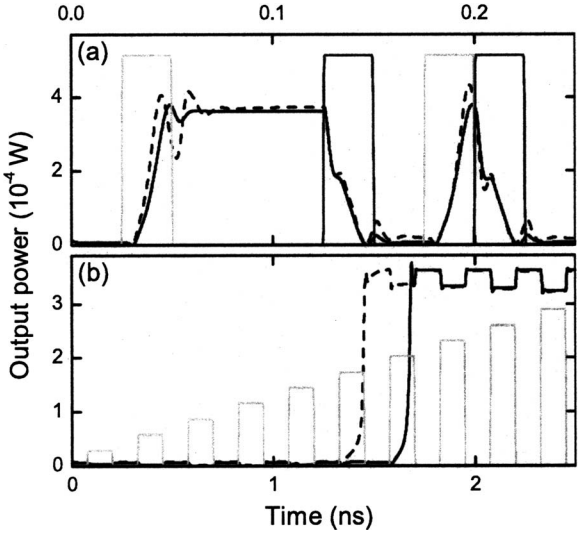


FIG. 2. (a) The power at the output port while set (light gray) and reset (dark gray) pulses are applied to the COFF. (b) The set operation is performed when the input power increases above 0.2 mW. The solid black curve is calculated for $\alpha_{\text{lef}}=0$ and the dashed curve for $\alpha_{\text{lef}}=0.5$. Note the different time scales in (a) and (b).

the system reaches equilibrium, the carrier density has returned to a static value, which is practically equal for the two states. The carrier density and optical power reach their steady state values fairly fast after the perturbation of the system ends, but complete phase relaxation takes longer.

The strong nonlinearity of the COFF, best seen in Fig. 2(b), suggests that the basic concept could also be used to realize other nonlinear functions. A similar construction without feedback has already been proposed as a way to realize a reamplifying, reshaping (2R) regenerator.[14] The nonlinearity offered by the interference and laser amplifiers alone is significantly enhanced by the presence of feedback.

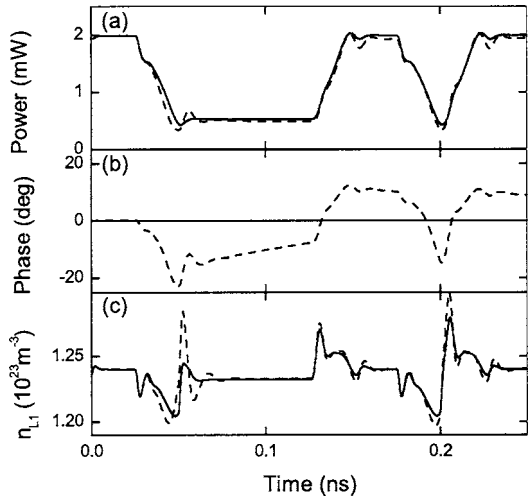


FIG. 3. (a) The output power and (b) the phase of the electric field of the laser mode and (c) the carrier density in laser $L_1$ for the set and reset pulses shown in Fig. 2(a). The input pulses affect the optical power of the laser mode through the carrier density and the gain. They also change the optical length of the cavity, which in turn alters the phase shift that the phase locking signal undergoes in the cavity. The device is, however, adjusted in such a way that the phase shift is roughly constant when the steady state is reached. The solid curve is calculated for $\alpha_{\text{lef}}=0$ and the dashed curve for $\alpha_{\text{lef}}=0.5$. Note that the power of the laser $L_1$ (or $L_2$, not shown) does not reduce to zero in either state, in contrast to earlier flip-flop constructions.

The approximately linear dependence of the maximum operating speed on the expression $\alpha_s$-$G_s$, found by small signal analysis of a single laser amplifier[14] and qualitatively verified by the numerical simulations, suggests that there is no fundamental reason why the operating speed could not be increased further. An interesting property is also the disappearance of the relaxation oscillations (also found in quantum cascade lasers,[15] with the small value of $\alpha_{\text{lef}}$ and high optical power-differential gain product.[14]

In conclusion, a method of providing the nonlinear feedback in an all-optical flip-flop by using coherent optical bias fields is introduced. The laser amplifiers of the flip-flop always operate above the threshold and therefore there is always a large photon population present in the laser mode. This allows a much faster response to incoming signals than in the conventional all-optical flip-flops where the nonlinearity is provided by the abrupt change in the output power taking place at the lasing threshold. Finding nonlinear interactions enabling optical computing, such as the one presented here, is one fundamental challenge for the research of optics.

The operational dynamics has been modeled by a set of rate equations describing the carrier densities and complex electric fields in each laser of the device. Although the rate equation model for phase locked lasers is well known and reasonably accurate, the results should be interpreted as a demonstration of concept rather than an in depth study of all the properties of the flip-flop. Still, the results do show promise of a fast integrated optical memory for specific small scale applications. Furthermore, despite the complexity of the structure, processing prototypes should be possible even with today's technology.

[1] M. Soljačić and J. D. Joannopoulos, Nat. Mater. **3**, 211 (2004).
[2] P. Russell, Science **299**, 358 (2003).
[3] V. R. Almeida, C. A. Barrios, R. R. Panepucci, and M. Lipson, Nature (London) **431**, 1081 (2004).
[4] K. Otsuka, Electron. Lett. **24**, 800 (1988).
[5] M. T. Hill, H. de Waardt, G. Khoe, and H. Dorren, IEEE J. Quantum Electron. **37**, 405 (2001).
[6] H. Kawaguchi, I. H. White, M. Offside, and J. E. Carroll, Opt. Lett. **17**, 130 (1992).
[7] F. Robert, D. Fortusini, and C. Tang, IEEE Photon. Technol. Lett. **12**, 465 (2000).
[8] G.-H. Duan, P. Landais, and J. Jacquet, IEEE J. Quantum Electron. **30**, 2507 (1994).
[9] P. Blixt and U. Öhlander, IEEE Photon. Technol. Lett. **2**, 175 (1990).
[10] M. Takenaka and Y. Nakano, IEEE Photon. Technol. Lett. **15**, 1035 (2003).
[11] Y. Liu, M. Hill, H. de Waardt, G. Khoe, D. Lenstra, and H. Dorren, Electron. Lett. **38**, 904 (2002).
[12] M. T. Hill, H. J. S. Dorren, T. de Vries, X. J. M. Leijtens, J. H. den Besten, B. Smalbrugge, Y.-S. Oei, H. Binsma, G.-D. Khoe, and M. K. Smit, Nature (London) **432**, 206 (2004).
[13] R. Lang, IEEE J. Quantum Electron. **18**, 976 (1982).
[14] J. Oksanen and J. Tulkki, IEEE J. Quantum Electron. **41**, 1075 (2005).
[15] R. Paiella, R. Martini, F. Capasso, C. Gmachl, H. Y. Hwang, D. L. Sivco, J. N. Baillargeon, A. Y. Cho, E. A. Whittaker, and H. C. Liu, Appl. Phys. Lett. **79**, 2526 (2001).